

Investigations on ballastless tracks in tunnel without reinforcement

Jia LIU

Track Technology, Schwihag AG, Tägerwilten, Switzerland

Email: jia.liu@schwihag.com

Stephan FREUDENSTEIN

Railway Infrastructure Research Group, Technical University of Munich, Munich, Germany

Email: stephan.freudenstein@vwb.bv.tum.de

ABSTRACT: Ballastless track systems have delivered an optimal performance in the past decades. This ideal comes from the Continuously Reinforced Concrete Pavement or the Jointed Plain Concrete Pavement in road design. It can be deduced that a well-proved system for road pavement is applicable to ballastless track design after certain modifications, which could save materials and simplify the construction work as well. In this paper, a feasibility study of ballastless track forms, in which neither reinforcement nor dowel bars shall be applied have been investigated using Finite Element Analysis. The results show that this idea is feasible in long tunnel with hard and stabile substructure, if a joint spacing less than 4 m can be realized. Meanwhile, these kinds of systems cannot be applied for track with soft substructures such as mass-spring-systems, in which continuous double-layer-reinforcement and sufficient thickness of the track concrete layer are required.

Keywords: Ballastless Track, Reinforcement, Finite Element Analysis

1 GENERAL

Ballastless track systems like Rheda 2000 have delivered an optimal performance in the past decades. In its standard application, the Track Concrete Layer (TCL) is continuously reinforced (Eisenmann 2002) in the centre of its cross section which has mainly the function as “crack-controller”: the maximum width of cracks and the distance between cracks in longitudinal direction depend on the percentage of reinforcement. It’s original ideal comes from the Continuously Reinforced Concrete Pavement (CRCP) with free cracking (Mönning 1952; Eisenmann 2002) in pavement design. Meanwhile, modifications of Rheda 2000 have been put into practice for metro lines as well (Hiliges und Bittner 1990; Von Wilken, Fleischer and Lieschke 2002). For example, a modified Rheda City metro line was built in Athena on soil base in 2007, in which the total longitudinal continuous reinforcement was replaced by dowel bars between two plain (un-forced) concrete slabs with a regular joint spacing of 3.25 m (Rossmann 2011), whose construction is in principle equal to the Jointed Plain Concrete Pavement (JPCP) in road design. This construction needs less material (steel) and the execution of the construction work can be simplified as well.

Generally, similar principles are used for the design of ballastless track systems and road pavements. Both constructions are multi-layer-systems under dynamic loading. The deformation of the concrete layer should be limited and the cracking behaviour has to be controlled strictly regarding to the long term behaviour of the concrete layer. Hence it can be deduced that a well-proved system for road pavement is applicable to ballastless track design after certain modifications, which are necessary to meet the special requirements in railway design. The modified Rheda-City metro line affirmed this statement. Beyond that, thoughts can be given that in case of simplified boundary conditions such as in long tunnels or stiff sub constructions without settlements and outdoor weathering influence, further modifications/simplifications can be done to reduce the initial investment and meet the local requirements as well.

In this paper, a feasibility study of three variations of ballastless track forms (figure 1), in which neither reinforcement nor dowel bars shall be applied have been investigated using Finite Element Analysis (FEA):

- Variation 1: direct pouring on tunnel invert with cant ≤ 35 mm and minimum of thickness $d_{min} = 300$ mm (Standard tunnel track STT-35 mm);

- Variation 2: direct pouring on tunnel invert with cant up to 150 mm and $d_{min} = 250$ mm (STT-150 mm);
- Variation 3: Vibration Isolation Track with cant ≤ 35 mm (VIT-35 mm): Prefabricated slabs on elastic vibration isolate mat with $d_{min} = 300$ mm (STT-VIT-35 mm).

Due to the fact that these track forms only consist of plain concrete slabs, they are designed for the application in long tunnel exclusively.

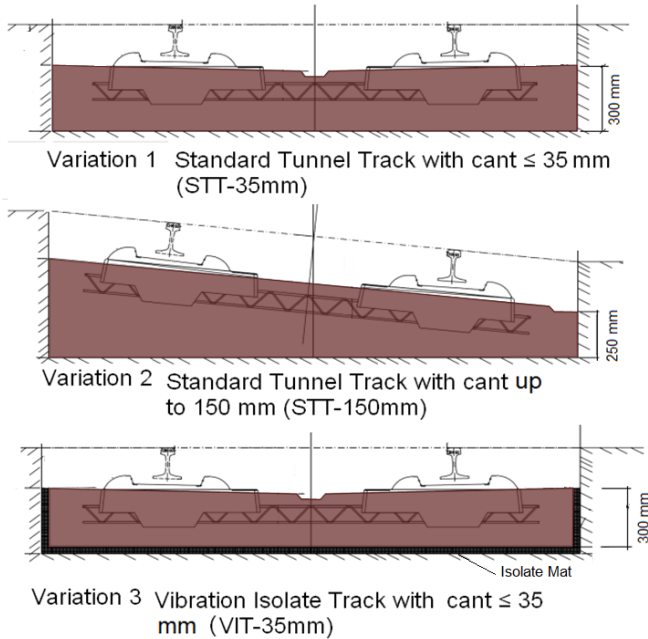


Figure 1. Three modified ballastless track forms for application in long tunnel

2 DEFINITIONS OF LOAD CASES FOR THE FINITE ELEMENT ANALYSIS

For a standard design of TCL, following load cases must be considered generally (Eisenmann and Leykauf 2007):

- Load case 1: shrinkage during and after hardening
- Load case 2: effects caused by outdoor weathering
- Load case 3: dynamic traffic loads
- Load case 4: restraint of extrinsic externally imposed deformation

Since no weather influence exists in a long tunnel ($L > 5$ km), load case 2 must not be taken into account. Load case 4 depends on the sub-construction, which is preconditioned as settlement-free in this study. Load case 1 and 3 are relevant for the further investigations. Due to the fact that the three variations consist of plain concrete slabs, the main goal of this study is to find a suitable length for joint spacing to avoid free cracking within the slabs. The maximum length of the TCL should be less than 20 times of the thickness of TCL in long tunnel (Freudenstein

2012). In the following, detailed analyses have been carried out in order to find a precise approach.

3 FINITE ELEMENT MODELLING

Finite Element Slab-Models with slab-lengths of 3.25 m, 3.9 m, 5.2 m, 7.8 m, 10.4 m and 13.5 m are generated (figure 2). To simulate the tunnel invert, springs are applied on the bottom of the 3D slab-models. The bedding modulus of the tunnel invert was set as 2 N/mm^3 for variation 1 and 2, which represents a very hard sub-structure without potential of deflection. For the simulation of variation 3 the bedding modulus of the isolate mat is assumed as 0.025 N/mm^3 for the first approach (DBS TL 918071 – 2006).

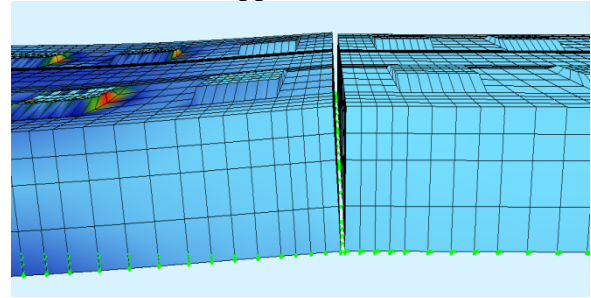


Figure 2. Detailed graph of joint spacing under traffic loading

To analyze the effect of traffic loads on joints, FE models consisting of at least two slabs with joints are generated as shown in figure 2. The load transfer within the joints is neglected in order to give a conservative result.

4 RESULTS AND DISCUSSION

4.1 Shrinkage during hardening

In general two effects lead to cracking during the hydration process of concrete: the heat of hydration and shrinkage (chemical bonded and physical evaporated loss of water). The heat of hydration is mainly depending on the type of cement and its strength class. Considering the compression forces caused by rapid increase of temperature, a major part of the compressive stress can be relieved by plastic deformation due to the low strength within the first hours. Tensile forces caused by cooling at the end of the hydration can be relieved by cracking on contraction joints. Shrinkage causes cracking especially in long tunnel because of the chimney-effect, which means an air passage with rapid drying effect on the surface of slabs. To avoid large hydration gradients in slabs, wet-treatments have major significance during the construction site work.

The shrinkage modulus of young concrete ϵ_s , which describes the material shrinkage behavior during hydration, is approximately 10 to 15E-5 (Eisenmann and Leykauf 2007). Shortening of concrete during dehydration, which results to tensile stresses within the concrete, can be simulated as a temperature load ΔT :

$$\Delta T = \epsilon_s / \alpha_T = -10 \text{ to } -15 \text{ K}$$

with

$\epsilon_s = 10 \text{ to } 15E-5$ [-], shrinkage modulus of young concrete;

$\alpha_T = 10E-6$ [1/K], thermal expansion coefficients of concrete.

A concrete of grade C30 has been chosen for the simulation. The material properties of C30 concrete can be found in the preset of the simulation tool. After defining the concrete grade and technical standard, all the material parameters about C30 are activated according to the given standard. In this case, C30 according to DIN 1045-1 (version: June 2012) has been defined. However, these values are only valid for concrete after hardening. For example, the young modulus, which is essential for calculating the tensile stress, increases during the hardening process. The value 3.3E5 N/mm² according to DIN 1045-1 can be achieved after around 28 days. For the calculation of wet concrete, a lower value of 2E5 N/mm² was taken into account. For the same reason, the maximum average tensile stress was given as 2 N/mm² instead of 3 N/mm² for wet concrete (figure 3). These values are a mean value for wet concrete C30 and were determined empirically by the German concrete industry.

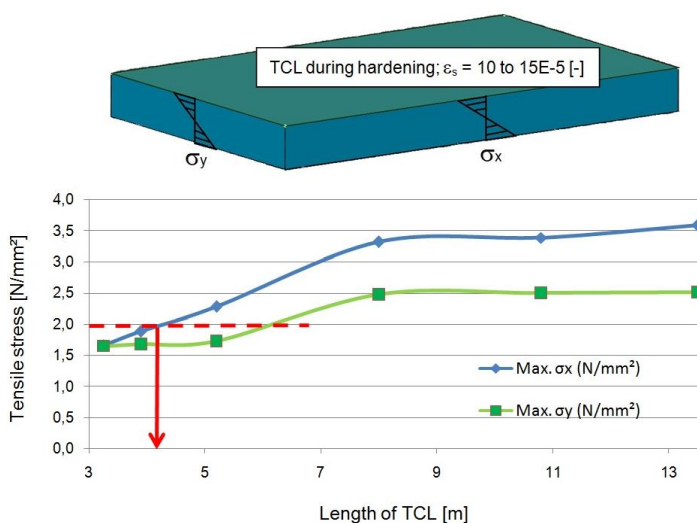


Figure 3. Maximum bending tensile stresses for different lengths of the segmented track plate – variation 1

According to the results shown in figure 3, the slabs should have a length less than approximately 4 meters to avoid free cracking in slabs in young age for variation 1. Variation 2 shows similar results. To avoid recurrence of similar charts, no results are shown for this variation.

Because the slabs in Variation 3 shall be prefabricated, no tensile stress is expected during hardening for this case.

4.2 Shrinkage after hardening

After hardening, the TCL shall be torn open completely at the contraction joints. Thus the slab ends become free to move at the joints. An equivalent temperature difference ΔT of - 25 K was applied to simulate the long-term shrinkage modulus ϵ_s of 25E-5 [-] (DIN Fachbericht 101-2003). The young modulus E for concrete C30 after hardening is taken as 3E5 N/mm² and its long-term tensile strength $f_{ct} = 3$ N/mm². It is obviously that the tensile stress in slabs cannot be higher than the maximum friction stress between slab and tunnel invert. The maximum friction ($\sigma_{max_friction}$) can be determined as (Freudenstein 2012):

$$\sigma_{max_friction} = \gamma * \mu * L / 2$$

with:

L: length of concrete slab,

γ : density of concrete,

μ : friction coefficient, for young concrete $\mu = 1.6$, for concrete after hardening $\mu = 0.8$.

(These values are a mean value and were determined empirically by the German concrete industry.)

The maximum tensile stress activated within the TCL is determined to 0.04 N/mm² with $\mu = 0.8$.

The displacement at one end of the plate (ΔL) can be calculated as:

$$\Delta L = \alpha_T * \Delta T * Lu / 2 - 0.25 * \gamma * \mu * Lu^2 / E = 0.48 \text{ mm}$$

with:

$\alpha_T = 10E-6$ [1/K], thermal expansion coefficients of concrete,

ΔT : equivalent temperature difference,

Lu: active length of concrete slab,

$E = 3E5$ N/mm², young modulus of concrete after hardening.

After duplicating of ΔL , the total joint opening can be determined to 1 mm for a slab with a length of 3.9 m.

According to these results, the tensile stress of 0.1 N/mm², which is caused by long-term shrinkage, can be neglected.

Generally speaking, the development of cracks can lead to additional impacts such as increasing of deflection and reducing the slab serviceability. One of the most important issues of designing slab track is to control the cracking process. However, in this investigation, the slabs shall be applied on very stiff tunnel invert. The change of deflection due to cracking can be neglected. The following calculations based on the assumption, that all the material has linear elastic properties. Cracking process and loss of concrete strength have not been taken into account.

4.3 Traffic load for a line with 17t axle load

The following calculation is based upon the FE Model with a joint spacing of 3.9 m. The following boundary conditions are given:

- Metro line or passenger dedicated line;
- static axle load $Q = 17$ t;
- Axle distance within bogie = 2 m;
- Dynamic stiffness of support point = 31.5 kN/mm;
- Support point distance: 0.65 m;
- Maximum speed: 200 km/h to 220 km/h.

The dynamic support point forces for the outer and inner rail are determined and shown in table 1.

Table 1: calculation of the traffic loads for variation 1 to 3

	Variation 1 and 2	Variation 3
dynamic stiffness of fastening system (support point, W300-1)	31.5 kN/mm	31.5 kN/mm
dynamic stiffness of substructure (bedding modulus)	2 N/mm ³	0.025 N/mm ³ DBS TL 918071
total dynamic stiffness of the track system	33.5 kN/mm	13.1 kN/mm
static support point force (Freudenstein 2012)	34.7 kN	29.4 kN
dynamic factor (Freudenstein 2012)	1.5	1.5
vertical load transfer factor (Freudenstein 2012)	1.2	1.2
dynamic support point force - outer rail	62.4 kN	52.9 kN
dynamic support point force - inner rail	41.6 kN	35.3 kN

A load pattern with a length of 4 times of the support point distance was applied as shown in figure 4 in order to simulate a train passage. To be on the safer side, load transfer to the joints was neglected.

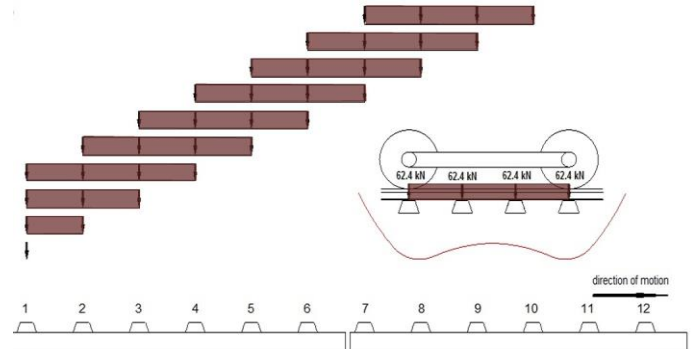


Figure 4: Loading patterns for the calculation of displacement of the TCL under dynamic loading

The displacements of variation 1 and 3 are shown in figure 5.

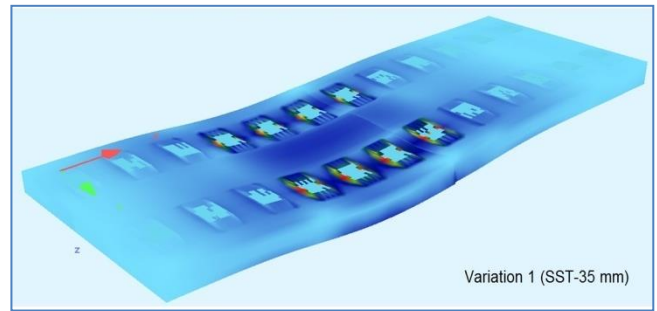
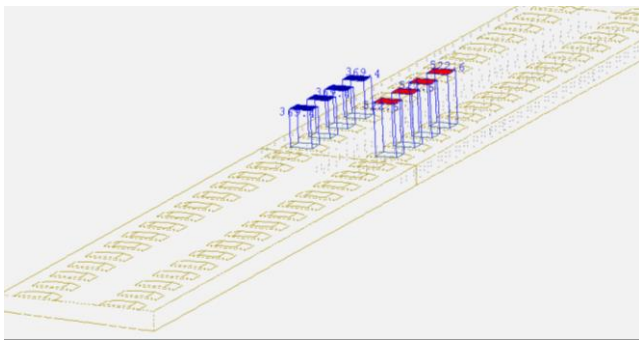


Figure 5: Displacements of variation 1 and 3 under dynamic loading

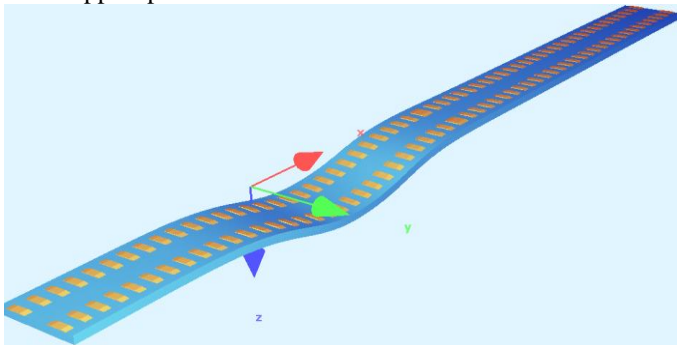
The maximum vertical deflection of the TCL in variation 1 and 2 was less than 0.1 mm (tunnel invert, no bending), which caused maximum tensile bending stresses of approx. 0.3 N/mm². The relative vertical displacement between two neighboring slabs of variation 3 was more than 3 mm, which causes high tensile stresses at the rail. To reduce the potential of relative movements and to increase the stability of the track, the slabs must be connected for example with continuous reinforcement.

4.4 Optimizing of variation 3

A FE model of a continuous TCL with a length of 25 meters (double-layer reinforced) is generated. The support point forces are applied to the model as shown in figure 6.



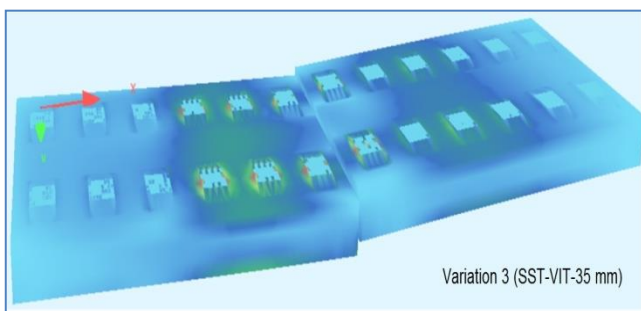
(a) dynamic loading on the FE model with 25 meters length - blue: support point forces at the inner rail; red: support point forces at the outer rail



(b) Deformation of the TCL under (a)

Figure 6: Calculation with double-layer reinforced TCL

The maximum vertical displacement of TCL caused by traffic loading was determined to 1.47 mm and 0.34 mm by dead load. The ratio of these two values was determined to $1.47 \text{ mm} / 0.34 \text{ mm} = 4.3$, which leads to high performance demands on the isolate mat and thus to early damage of the elastic structure (recommended ratio: 2). Hence no good long term behavior of the track system is expectable in this case.



Further optimization was undertaken to decrease the ratio: The thickness of the slabs is increased from 50 cm to 90 cm and the bedding modulus of the isolate mat is increased from 0.025 N/mm^3 to 0.1 N/mm^3 (DBS TL 918071 -2006). The results for $C = 0.1 \text{ N/mm}^3$ and 0.05 N/mm^3 are shown in figure 7.

Relation between displacements, thickness and bedding modulus

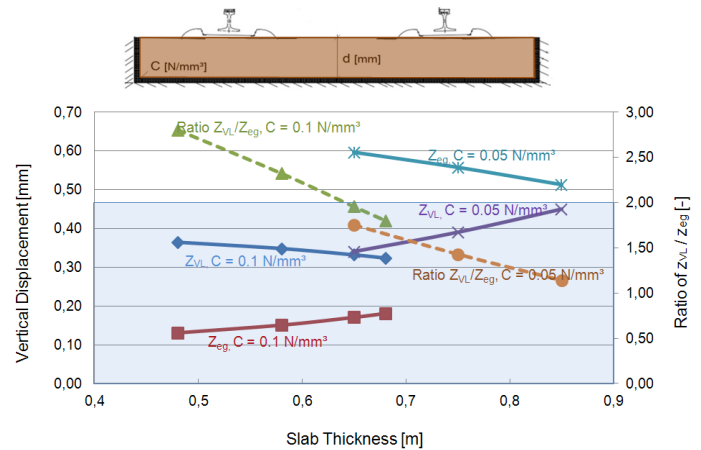


Figure 7: Relation between slab displacements, thickness and bedding modulus (Z_{VL} : vertical displacement resulted by traffic loads; Z_{eg} : vertical displacement resulted by dead loads; Ratio Z_{VL} / Z_{eg} : ratio between Z_{VL} and Z_{eg})

To meet the recommended ratio of 2, the minimum of slab thickness is determined to 65 cm while C is 0.1 N/mm^2 . For systems with reduced bedding modulus, slabs with bigger thickness are required.

5 CONCLUSIONS

A feasibility study using finite element method is created to investigate the practicability of three alternative designs of the standard Rheda 2000 ballastless track system in tunnel, in which neither reinforcement nor dowel should be applied:

- Variation 1: direct pouring on tunnel invert with cant $\leq 35 \text{ mm}$ and a minimum TCL thickness $d_{min} = 300 \text{ mm}$ (STT-35 mm);
- Variation 2: direct pouring on tunnel invert with cant up to 150 mm and $d_{min} = 250 \text{ mm}$ (STT-150 mm);
- Variation 3: pre-fabric-produced slabs on elastic vibration Isolate mat with cant $\leq 35 \text{ mm}$ and $d_{min} = 300 \text{ mm}$ (STT-VIT-35mm).

The following essential conclusions can be drawn:

Variation 1 and 2 are feasible in practice if a joint spacing less than 4 m can be realized. Since no reinforcements and dowel bars are designed, sufficient wet-treatment after cast and the timely manufacture of joints have major significance and influence to the long-term quality of the track.

For Variation 3, the displacements in this system under dynamic loading are too big due to the unconnected slabs and soft bedding. This leads to high performance demands on the isolate mat and conse-

quently to early damage of the rubber structure. Further, the thickness of slabs is not sufficient to work as a mass-spring-system. To achieve a good long-term behavior, continuous double-layer-reinforcements shall be applied. Meanwhile, the thickness of TCL and the bedding modulus of the elastic mat shall be designed accurately to achieve the isolate function. Examples are given in the text.

6 REFERENCES

- DBS TL 918071, "Deutsche Bahn - Standard für die technischen Lieferbedingungen von Unterschottermatten zur Minderung der Schotterbeanspruchung", Dezember 2006.
- DIN Fachbericht 101, "Einwirkung auf Brücken", Ausgabe März 2003.
- Eisenmann J., Leykauf G., "Verkehrsflächen aus Beton", *Betonkalender 2007*. Ernst & Sohn, Berlin.
- Eisenmann J., "Redundanz der Festen Fahrbahn Rheda", *Eisenbahningenieur* 53 (2002), Heft 10. pp. 13-18.
- Eisenmann, J., Leykauf, G., "Feste Fahrbahn für Schienenbahnen", *Betonkalender 2000*. Ernst & Sohn, Berlin.
- Freudenstein, S., Script "railway design", Script "concrete pavement design", *Chair and Institute of Road, Railway and Airfield Construction, Technische Universität München* 2012
- Hilliges S.D., Bittner W., "Feste Fahrbahn Rheda-Sengeberg", *Eisenbahntechnische Rundschau* 39 (1990), Heft 3, pp. 155-160.
- Mönning, E., "Kontinuierlich bewehrte Betonstraßen aus den USA", *Straße und Autobahn* 3 (1952), H. 10, pp. 344-347 und H. 12, pp. 414-417.
- Rossmann H.C., Panagiotopoulos K., "The Athens Metro – quiet renaissance of an underground track system", *RTR Special/Slab Track and MRT/LRT*. 2011
- Von Wilken A., Fleischer W., Lieschke H., "Herstellung Feste Fahrbahn Rheda, Bauart Walter-Heilit mit Zweiblockschwelle auf NBS Köln-Rhein/Main", *Eisenbahntechnische Rundschau* 51 (2002), Heft 4, pp.172-182.